Chapter 5

Combined ligand-based and structure-based design of anti-Alzheimer agents targeting Phosphodiesterase 9A

5.1 Introduction

Dr. Henry Hyde Salter first attributed the bronchodilatory effects of caffeine in 1886. The stimulant was later found to be a non-selective inhibitor of the Phosphodiesterases enzymes. In 1958, Earl Sutherland and Ted Rall isolated the heat-stable nucleotide cyclic adenosine monophosphate (cAMP), from liver extracts, that was followed by the discovery of cyclic guanosine monophosphate (cGMP), in urine of rat. The study also recognised that PDE is capable of hydrolyzing cAMP[97].

Phosphodiesterases are a diverse superfamily of intracellular enzymes responsible for the breakdown of phosphodiester bonds in various cyclic nucleotides thereby regulating signal transduction. PDE enzymes play a crucial role in signal transduction at the cellular level via the two important secondary messenger molecules, cGMP and cAMP.

PDEs are classified into eleven subtypes, distributed over 40 isoforms [98, 99]. The enzymes function by hydrolyzing two secondary messengers i.e., cyclic 3, 5 adenosine monophosphate (cAMP) and 3, 5 cyclic guanosine monophosphate (cGMP) into 5'-AMP and 5'-GMP, respectively [100, 101]. These are ubiquitous in the human body; therefore, act as therapeutic targets for various diseases including erectile dysfunction, respiratory disorders, congestive heart failure, and AD.

Intercellular secondary messengers, i.e., adenosine-3′, 5′-cyclic monophosphate (cAMP) and guanosine-3′, 5′-cyclic monophosphate (cGMP) are involved in the regulation of the activity of various neurotransmitters and inflammatory mediators. The messengers play key role in numerous physiological processes viz. inflammation, immunological reaction, vascular resistance, cardiac output, gastrointestinal motility, neuroplasticity, reproduction, and vision [102]. PDE 1, 2, 3, 4, 5, and 9 inhibitors are also reported to affect memory and cognition in several models of AD, including aged animals [103, 104]. Furthermore, studies involving PDE3 or PDE9 inhibitors, in individuals with MCI or AD, are currently in phase II clinical

trials [97]. Expression of certain enzymes of PDE subfamilies were s shown to have been upregulated in AD brain, as compared to the control brain. PDE inhibitors induce an increase in the levels of cAMP and cGMP, leading to the activation of AC/cAMP/PKA or NO/cGMP/PKG signalling pathway, thereby augmenting the levels of the cAMP response element-binding protein (CREB) and subsequently increasing the synaptic transmission and decreasing the cognitive deficit.

Phosphodiesterase 9 (PDE9) has the highest affinity for cGMP amongst the various PDE subfamilies. PDE9A is the only isoform of PDE9 which is expressed throughout the brain, especially in the cerebellum, cortex, hippocampal pyramidal cell layer, and all over the striatum. Biological effects of PDE9 inhibitors have been explored in several AD animal models and thus making it a potential target to treat memory deficits related to aging and neurodegenerative disorders such as AD. However, a relatively low number of PDE9 inhibitors have been developed in so far, in comparison to subfamilies PDE4 and PDE5.

PDE9 inhibitors, BAY 73-6691 and PF-04447943 produced significant enhancement in the memory performance in social recognition tasks, object recognition tasks and Morris water maze experiments. BAY 73-6691 also exhibited prolonged early and late long-term potentiation (LTP) as compared to the AChE inhibitor donepezil, and transformed early LTP into late LTP. PDE9 inhibitors, BI-409306 and PF-04447943, have been subjected to AD clinical trials based on the results obtained in preclinical studies. Owing to its elevated expression in the brain and the established role of cGMP in the regulation of synaptic function, a potent (IC_{50} = 12 nM), selective, and brain-penetrant (logBB = −0.4) PDE9A inhibitor, PF-4447943, was developed by Pfizer[105]. The compound showed an elevation of brain cGMP levels *in vivo* and a selectivity ratio of 1:78 for PDE9A over the other members of PDE family, including isoforms and splice variants.

The role for the enzyme in regulation of monoaminergic signalling pertaining to the sensory

processes and memory could be substantiated from its *in vivo* effects. Regulation of cGMP based neuronal signalling downstream to numerous neurotransmitter systems is maintained via PDE9A activity, implicating that its inhibition could have an advantageous effect in the treatment of psychiatric and neurodegenerative diseases. However, a phase 2 clinical trial carried out in 2010 on subjects with mild to moderate AD failed to deliver favourable outcomes, casting a shadow on the effectiveness of PDE9A inhibitors in the treatment of AD.

Memory function restorative strategies represented by the inhibition of phosphodiesterase (PDE) activity using small molecule inhibitors via elevation of 3′,5′-cyclic adenosine monophosphate (cAMP) and 3′,5′-cyclic guanosine monophosphate (cGMP) and/or influencing nitric oxide (NO) levels could be a fruitful approach. Many of the reported pathways, relevant to the learning function in animal models of AD, are linked to PDE9. Therefore, designing inhibitors for the same might provide a significant breakthrough in terms of a disease modifying therapy for AD.

5.2 Materials and methods

5.2.1 Selection of protein structure

The crystal structure of the PDE9A catalytic domain complexed with an orally bioavailable small molecule inhibitor (PDB id – 9Q9) was obtained from PBD (https://www.rcsb.org/ structure/6a3n). The protein was selected out of a total of 25 crystal structures of PDE9A (*Homo sapiens*) available at the PDB. It had a resolution of 2.60 Å, R-value (free) of 0.280 and consisted of two chains (A, B; 322 residues). Further, 6A3N was the best resolved structure complexed with its inhibitor (9Q9), the latter obeying most of the drug likeliness rules. Ramachandran plot of the protein showed zero groups in the disallowed region and an overall core part of 93.3%. The protein had an overall quality factor of 98.0with 86. 86.02% of the residues having average 3D-1D score ≥ 0.2.

5.2.2 Pharmacophore Modeling

Pharmacophore models were developed by using Phosphodiesterase 9 receptor (PDB ID: 6A3N) with 9Q9 as a co-crystallised ligand (https://www.rcsb.org/). The pharmacophore-based virtual screening was performed on the Pharmit server. The interactions between the enzyme and 9Q9 were studied on BIOVIA Discovery studio and the interacting pharmacophoric features i.e., hydrogen bond acceptor (HA), hydrogen bond donor (HD), hydrophobic group (HY) and aromatic ring (A) were used to generate pharmacophore models. Seven different models were developed by using the above pharmacophoric features [106, 107]. Zinc15 library comprising of 123,399,574 conformations of 13,190,317 compounds, was used to search the virtual hits. Further, the search was being restricted to one conformer per molecule and one molecule per hit.

5.2.3 Molecular properties filter

KNIME® analytics platform ver. 4.3.0 was used to filter the previously obtained virtual hits for drug likeliness [9]. A workflow consisting of various KNIME nodes, including an SDF reader (for reading molecular input structures) was designed to filter and screen the molecules. Calculation of the molecular properties of ligands was carried out via the descriptor calculator node provided by RDkit. Ligands featuring one or less than one violation were selected (by using numerical row filter) to undergo further studies. Pharmacological parameters such as drug-likeness, BBB permeation, and Lipinski's ruleoffive formed the criteria for ligand filtration. Drug molecules targeting the central nervous system (CNS) must be capable of passing through the blood-brain barrier (BBB), which is chiefly composed of endothelial cells making up the brain capillaries[108]. Lipinski's rule-of-five was formulated based on the wide array of available information pertaining to the approved drug molecules and was employed to assess the drug-likeness of the molecules to qualify as a prospective orally active agent.

5.2.4 Pan-assay interference compounds (PAINS) filter

PAINS compounds can affect biochemical assay by presenting as reasonable factors for drug development in most individual studies. These may pass the criteria for screening selectivity designed to eliminate false positives by interfering photometrically or in some other direct way with the assay signaling due to the presence of specific functional groups and their combinations [109, 110]. The functionalities that usually interfere with bioassay are biological nucleophiles such as thiols and amines, metal chelators, proteins which are photoreactive and are included in PAINS[111]. The molecules that might act as potential PAINS candidates were separated by using data obtained from the SWISS ADME server.

5.2.5 Protein Preparation

The X-ray diffraction-based protein 3D model for human Phosphodiesterase 9 receptor (PDB ID: 6A3N), having a resolution of 2.60 Å, was obtained from protein data bank (https://www.rcsb.org/structure/6A3N). The protein was complexed with ligand 9Q9 having IC_{50} value of 8.7 nM. The protein of interest was processed using AutoDock Tools 1.5.6 to merge non-polar hydrogens, assign the type of atom and Gastieger's charges. All the water molecules within the protein structure were examined and subsequently removed. Further, the bound ligands and ions were removed and the protein was converted into an AutoDock compatible format, i.e., PDBQT [16].

5.2.6 Ligand Preparation

The hits obtained, after the molecular properties and PAINS filtration, were drawn using chem3D and saved in SDF file format. Open Babel was used to convert the SDF files into pdbqt format. Energy minimisations for the selected compounds were carried out to resolve the geometry and remove steric clashes and overlapping atoms. Energy minimization is a process that minimizes the potential energy of a system to determine its proper molecular arrangement

in space. It is crucial for proteins and ligands that the steric clashes between atoms are removed, accuracy of the docking process is improved the by developing a reasonable starting pose, and identifying the correct orientations of ligands when bound to a protein. This helps to ensure the protein and ligand are in a stable conformation and enhance the accuracy of the docking process. All the minimizations were executed using Open Babel 3.1.1 [17]. The ligands with minimized energies were then converted into AutoDock compatible format, i.e. PDBQT [16]. Consequently, all the energy minimized ligand molecules were subjected to molecular docking studies.

5.2.7 Grid generation for molecular docking

Protein–Ligand Interaction Profiler (PLIP) was used to identify the residues involved in non-covalent interactions with 9Q9 in the selected PDB file. The identified residues were taken as reference points to build a grid box around the active site. The grid generation was performed by using Autogrid 4.0 of the Autodock Tools 1.5.6 to calculate the grid maps of interaction energies with various types of atoms present in the ligands (A, C, HD, NA, N, OA, S, Br, Cl and I). Further, the developed grid was validated by redocking 9Q9 with randomised coordinates. The redocked pose was evaluated by determining RMSD corresponding to the heavy atoms with the co-crystallised structure of 9Q9. A grid box with grid dimensions set to 100*100*120, and a grid point spacing of 0.375 Å was employed for grid map calculations.

5.2.8 Virtual screening and molecular docking

The docking study was performed in three steps viz. high- throughput virtual screening (HTVS), standard precision, and extra precision via PyRx 0.8 and Autodock 4.2.6 using the Lamarckian genetic algorithm (LGA). Virtual screening involved the use of computational techniques to sift through vast chemical databases, optimizing focused combinatorial

libraries, as well as swift evaluation of massive chemical libraries whereby it acted as a filter to inform the selection of likely drug candidates [20]. Identifying potent hits that yield a particular pharmacological profile is the ultimate goal of virtual screening. PyRx 0.8 was employed to perform virtual screening via high-throughput docking modules [21], subsequently, the screened ligand molecules underwent standard precision (SP) and extra precision (XP) docking [22]. Compound library thus formed, was docked against the PDE9A enzyme structure. Discovery Studio Visualiser (DSV) was utilized for post-docking analysis and visualization.

5.2.9 ADMET property

ADMET profile of a compound is an important aspect of its clinical efficacy. The PreADMET server provides a user-friendly web interface to predict various ADME and toxicity parameters [23]. The absorption of the drug is a limiting factor for its bioavailability and response. A drug is considered well absorbed if it shows human intestinal absorption (HIA) above 70%. Since the 1990s, the pharmaceutical sector has adopted the philosophy "fail early, fail cheap", which comprehends that potency is not the only property that matters. This has resulted in the integration of *in silico* and *in vitro* absorption, distribution, metabolism, excretion, and toxicity (ADMET) filters in the initial drug discovery and development stages. Such strategy has brought about a remarkable decline of ADME issues-related project termination rates [15].The compounds obtained from the third stage of docking were analysed for ADME properties and toxicity. The ADME properties were obtained from the SwissADME server (http://www.swissadme.ch/) and the toxicity prediction was made through the PreADMET server (https://preadmet.bmdrc.kr/toxicity/).

5.2.10 Molecular dynamics

Select compounds, fulfilling ADMET criterion, were subjected to MD simulation. Molecular function and intermolecular interactions of the biomolecules rely on the dynamics of the latter, which are perpetually in motion. Molecular dynamics (MD) simulations provide a window to view the biomolecules in action and to understand how they might respond when perturbed at the atomic level. MD simulations help to predict how each atom in a protein or ligand (or in other complex systems) move over time under general physics/classical mechanics governed interatomic interactions.

A huge gamut of key biomolecular processes such as conformational change, ligand binding, and protein folding can be captured to reveal the positions of all of the atoms resolved to femtosecond scale. All in all, MD and docking approach greatly complement each other in the drug discovery process.[112]

MD simulation run of 100 nanoseconds was performed on the protein 6A3N complexed with each of the selected compounds following the docking studies using Maestro–Desmond Interoperability Tools (Schrödinger, LLC, New York). The refined system was solvated in a cubic box containing TIP3P water molecules to form an aqueous environment and 0.15 M NaCl was added to mimic the ionic strength inside the cell under physiological conditions. The run was performed at a temperature of 310 K, pressure of 1 bar at constant volume and temperature (NPT ensemble) under periodic boundary conditions. Prior to running the MD simulation, the system was relaxed, following which the MD simulations were executed at 100 ns. Subsequently, the results were evaluated through studying the RMSD interactions. RMSD plots for the Cα atoms were generated for both the protein as well as the ligand-bound protein for each compound to understand the relative stability of ligand molecule within its binding pocket using Maestro (Schrödinger, LLC, New York).

MD simulations, carried out to evaluate chemistry at the molecular level, were performed for **ZINC000001305675** and **ZINC000000377099** complexes using the Desmond package of Schrodinger [113].

5.3 Results & discussions

5.3.1 Pharmacophore modeling and virtual screening

The crystal structure of a small molecule inhibitor (9Q9) complexed with the PDE9 receptor (PDB id – 6A3N), of optimum resolution 2.60 Å, was taken in the study. The structure of this protein was resolved by the X-ray diffraction method. The ligand, 9Q9 is a Pyrazolopyrimidinone derivative and a potent inhibitor of the PDE9 enzyme. Seven pharmacophoric models were derived from the cocrystallized structure of the enzyme and the inhibitor to obtain 7498, 2597, 5515, 4480, 2691, 2370, and 12403 virtual hits, respectively (**Table 5.1**). A combination of different pharmacophoric features such as hydrogen bond donor (HD), hydrogen bond acceptor (HA), aromatic ring (A) as well as the hydrophobic group (HY) were used in the pharmit server (http://pharmit.csb.pitt.edu/) to create models containing multiple pharmacophoric features [114]. The number of hits was restricted to one conformer per molecule and one molecule per hit as selection criteria for ZINC database screening[115]. A range of virtual hits were obtained from all seven models, as described in the table (**Table 5.1**) with their pharmacophoric features involved. The number of hits obtained were considerably huge to perform individual molecular docking, so a further reduction of the virtual hits was performed using molecular property and PAINS filters.

Table 5.1 Features of pharmacophore model of PDE9 enzyme (H: Hydrophobic, A: Hydrogen bond acceptor, D: Hydrogen bond donor)

S.No.	Model No.	No. of Features	Features	No. of Hits
1	1	5	1HD,2HA,2Hy	7498
2	2	4	1HD,3HA,1Hy	2597
3	3	5	4HA,1Hy	5515
4	4	5	1Ar,1HD,1HA,2Hy	4480
5	5	5	1Ar,1HD,2HA,1Hy	2691
6	6	5	1Ar,1HD,3HA	2370
7	7	4	1HD,2HA,1Hy	12403

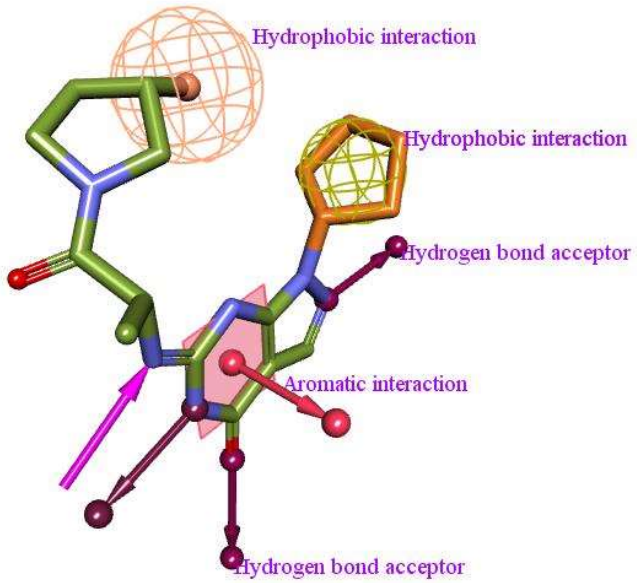

Figure 5.1 Pharmacophore model developed from the PDB file of PDE 9A co-crystallised with 9Q9

5.3.2 Drug likeliness and molecular properties filter

Drugs are, by far a vaguely specified class of chemical entities, which, other than displaying affinity to the intended therapeutic target, must also fulfil certain criteria *viz.,* bioavailability, efficacy, while being devoid of chronic and/or acute toxicity, mutagenicity etc.

"Drug likeness", often described to be a proxy for oral bioavailability, is a concept used to loosely define the criterion for a molecule, in the initial stages of drug discovery, in order to be taken up for further studies. Simple physicochemical properties such as molecular weight, polarity and hydrophobicity have an impact on the *in vivo* molecular behavior, metabolic stability, permeability as well as transport characteristics of a molecule.

As simple drug-like properties, the molecular mass, number of heavy atoms, number of rotatable bonds, number of aromatic rings, number of chiral centers, lipophilicity [e.g., octanol-water partition coefficient (logP), and for ionizable compounds, logD], polar surface area and topological surface area, and the number of hydrogen bond donors and hydrogen bond acceptors are the main developmental parameters analyzed during the lead to clinical candidate process.

Certain sets of rules/filters had been developed to define acceptable limits of molecular properties based on their shared similarities across all the approved oral drug candidates. The filters help to screen out some of the molecules from the libraries, thereby, reducing the risk of attrition at the advanced drug discovery stages down the line. The most prominent drug-likeness filter among all is the Lipinski proposed "Rule-of-Five". The rule-of-five or Ro5, originally developed by Pfizer, employs drug-likeness filters to filter out the compounds based on molecular weight (≤500), LogP (≤5), H-bond donors (≤5), and H-bond acceptors (≤10).

Filtering extensive databases based on suitable molecular properties, prior to docking based screening in order to reduce the computational efforts and eliminate unnecessary compounds, is a common practice. KNIME workflow was employed to carry out the drug likeliness filtering.

The workflow was designed so as to calculate cLogP, molecular weight, number of rotatable bonds, number of hydrogen bond donors and number of hydrogen bond acceptors of each

compound. Physicochemical properties of approved CNS active drugs dictate the acceptable limits for the above-mentioned properties (**Table 5.2**) [30].

KNIME analytics platform was used to design a workflow to filter the selected compounds for drug likeliness. Several molecular properties of the compounds including molecular weight, number of rotatable bonds, xLogP, Topological Polar Surface Area (TPSA), number of hydrogen bond acceptors (HBA) and number of hydrogen bond donors (HBD) were calculated by using this workflow.

Lipophilicity is a vital measure for CNS penetration and increased lipophilicity might lead to increased CNS penetration. Compounds, deviating from the 'Lipinski's Rule-of-Five' and the 'REOS' filters, obtained from the virtual screening were filtered out using KNIME analytics platform with the criteria mentioned in **Table 5.2**.

Table 5.2 The default parameters used for the REOS filter

Criterion	limits
Molecular weight	Between 200 and 500
LogP	Between -5.0 and +5.0
H-bond donor count	Between 0 and 5
H-bond acceptor count	Between 0 and 10
Formal charge	Between -2 and +2
Rotatable bond count	Between 0 and 8
Heavy atom count	Between 15 and 50

TPSA is another significant predictor of BBB penetration. Usually, the TPSA value of CNS active drugs is lower than other classes of drugs. Thus, 1,129 compounds, out of 30,000 virtual screening results passing the filters/parameters, were expected to be CNS active. The features

considered for molecular properties filtration included drug-likeness, BBB permeation, and Lipinski's rule-of-five. A drug molecule targeting CNS must have optimum lipophilicity to permeate BBB. The BBB is a semi-permeable barrier made up of endothelial cells and the cells form brain capillaries that tightly regulate the brain's diffusion and ion exchange process [116]. Lipinski rule of five has four parameters, i.e., the molecular mass should be less than 500 Da, hydrogen bond donors should not be more than 5, hydrogen bond acceptors must be limited to 10 and log P should not be more than 5 of a hit. It is an important criterion which shows the absorption and permeability capability of a drug molecule [117]. The molecular properties filtration reduced the number of hits to a few hundred, as shown in the **Table 5.3**.

Table 5.3 Results obtained after molecular properties filtration

Model No.	Features	No of features	Hits before filtration	Hits after filtration
1	1HD,2HA,2Hy	5	7498	290
2	1HD,3HA,1Hy	5	2597	82
3	4HA,1Hy	5	5515	236
4	1Ar,1HD,1HA,2Hy	5	4480	117
5	1Ar,1HD,2HA,1Hy	5	2691	67
6	1Ar,1HD,3HA	5	2370	77
7	1HD,2HA,1Hy	4	12403	281

5.3.3 Pan-assay interference compounds (PAINS) filter

A molecule with disruptive reactivity acts as a drug but provides false-positive results in various assays, usually referred to as Pan-assay interference compounds (PAINS). The false-positive results could be attributed to the presence of fluorescent or chromophoric groups giving positive results even in the absence of the particular protein. The nonspecific

interactions of the compounds with several biological targets also lead to interference in biological assays by means of false-positive results. Hence, a PAINS filter is required to remove such interfering hit molecules from the data obtained through the Swiss ADME server.

Table 5.4 Results obtained after PAINS filtration

Model No.	Features	Hits before PAINS Filtration	Hits after PAINS Filtration
1	1HD,2HA,2Hy	290	286
2	1HD,3HA,1Hy	82	80
3	4HA,1Hy	236	234
4	1Ar,1HD,1HA,2Hy	117	113
5	1Ar,1HD,2HA,1Hy	67	66
6	1Ar,1HD,3HA	77	77
7	1HD,2HA,1Hy	281	272

5.3.4 Protein and ligand preparation

The selected 3D model of Phosphodiesterase 9 receptor bearing the PDB ID - 6A3N was converted into a pdbqt file after removal of water molecules, addition of polar hydrogens and Kollman charges to the PDB structure of protein using Autodock Tool-1.5.6 [118, 119]. The ligand preparation step was performed using chem3D and Open Babel software. Chem3D was used to draw the ligands' structure in 3D and was followed by energy minimization. Subsequently, PAINS filtration was carried out and Open Babel was used to convert the structures from SDF to pdbqt format.

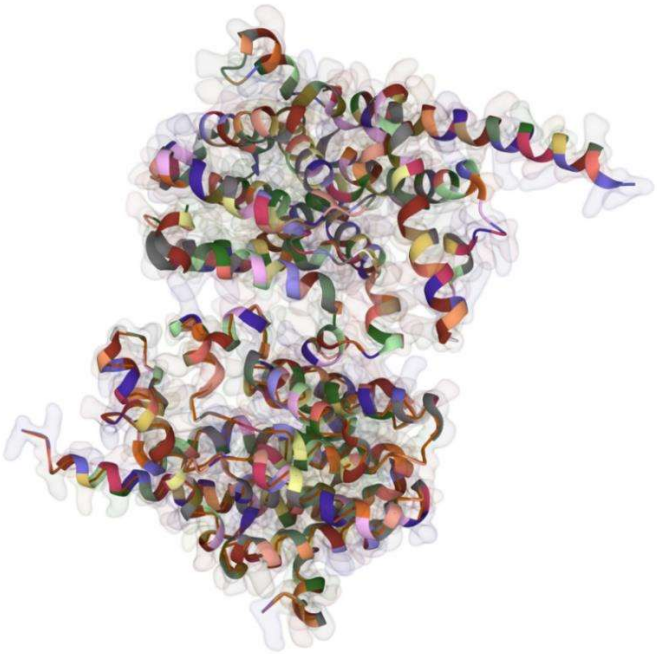

Figure 5.2 3D structure of phosphodiesterase 9A (6A3N)

5.3.5 Grid generation for molecular docking

The grid generation defines the binding sites in a receptor where ligand interaction might occur and is an essential step that needs to be performed before molecular docking [120]. Therefore, grid generation was performed with grid dimensions 56*62*54 and 0.375 Å grid point spacing to surround the binding sites, i.e., Phe 456 amino acid residue. Phe 456 amino acid residue is essential for ligand binding with phosphodiesterase 9 receptor as a potent inhibitor [121]. Moreover, a grid generation would produce reproducible and valid results for virtual screening using molecular docking.

5.3.6 Virtual screening and molecular docking

Virtual screening through molecular docking is one of the most essential steps in the process of drug design to evaluate the binding affinity of the virtual hit compounds to the target protein[122]. In addition, the screening techniques assist to identify potent compounds in order to discover inhibitors that resemble the co-crystallized ligand structure or other innovative

leads. Autodock Vina, designed and implemented by Dr. Oleg Trott, is one of the most dependable tools available for molecular docking and virtual screening. It is a multi-faceted, high-throughput, and increasingly accurate device for virtual screening. The functioning of this software requires AutoDockTools and command prompt [123]. It uses a new scoring function to develop an efficient optimization approach for predicting protein-ligand affinity. It may also execute calculations in parallel on a single system utilizing several CPUs to speed up the process [124]. AutoDock Vina uses a unique combination of empirical scoring function, a knowledge-based function which is inspired by the X-score function and is different from the AutoDock scoring function [125, 126]. To sort out and reduce the numerous hits from large databases, the scoring functions act as both rapid as well as reliable systems. 110 ligands were screened out of approximately 1000 ligands with binding energy of less than -9 kcal/mol via virtual screening. Further, 5 ligands, out of total 13, were selected for analyzing the protein-ligand interactions with the binding energy ranging from -9.75 to -10.09 kcal/mol.

$$V = W_{vdw}\sum_{i,j}\left(\frac{A_{ij}}{r_{ij}^{12}} - \frac{B_{ij}}{r_{ij}^{6}}\right) + W_{hbound}\sum_{i,j}E(t)\left(\frac{C_{ij}}{r_{ij}^{12}} - \frac{D_{ij}}{r_{ij}^{10}}\right) + W_{elec}\sum_{i,j}\frac{q_i q_j}{e(r_{ij})r_{ij}} + W_{sol}\sum_{i,j}\left(S_i V_j + S_j V_i\right)e^{\left(-r_{ij}^2/2\sigma^2\right)}$$

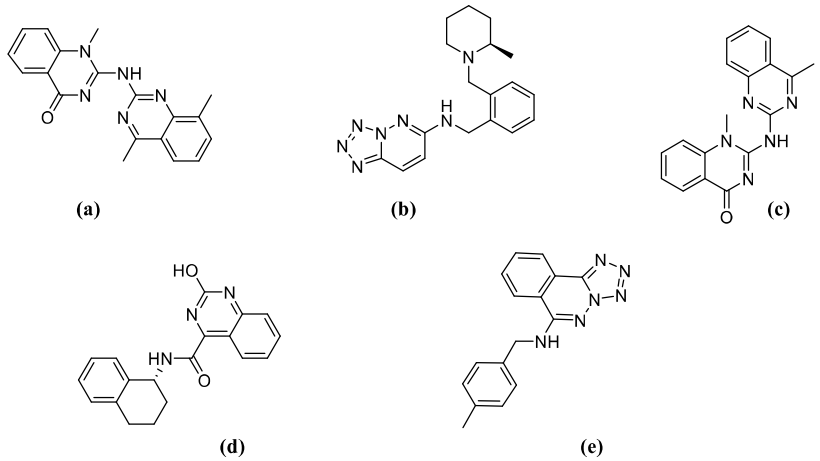

Figure 5.3 Molecular structure of final compounds (a) **ZINC000001305675** (b) **ZINC000052245110** (c) **ZINC000000377099** (d) **ZINC000426406009** (e) **ZINC000020579927**

Table 5.5 Docking results displaying lowest binding energy of ligands against PDE9 receptor

S.No.	Model No.	ZINC ID	Binding Affinity
1	1	**ZINC000001305675**	-10.9
2	1	**ZINC000000377099**	-10.3
3	7	**ZINC000052245110**	-10.2
4	1	**ZINC000426406009**	-10.1
5	7	**ZINC000020579927**	-10.1
6	6	**ZINC000101501126**	-9.9
7	1	**ZINC000012610356**	-9.8
8	1	**ZINC000004334781**	-9.8
9	2	**ZINC000101483378**	-9.8
10	3	**ZINC000021658485**	-9.7
11	4	**ZINC000000191941**	-9.7
12	7	**ZINC000052244890**	-9.7
13	7	**ZINC000052244891**	-9.7

The ligand **ZINC000001305675** displayed hydrogen bonding with ASP402 and MET365, while ILE403 took part in π − σ interactions. PHE251 showed π – π stacking interaction, while, PHE456 and LEU321 formed π − alkyl interactions with the aromatic ring of the ligand. (**Figure 5.4** (**a**)). Ligands **ZINC000001305675** and **ZINC000000377099** displayed similar bonding since the core structures were identical and being part of the same pharmacophore model. Hence, **ZINC000000377099** displayed hydrogen bonding with ASP402, while ILE403 took part in π − σ interactions. Additionally, HIS206, HIS252 and PHE456 showed π − π stacking interactions, together with PHE251, while, LEU321 formed π − alkyl interactions. (**Figure 5.4** (**b**)). **ZINC000052245110** formed π − π stacking with PHE456 and PHE441, π − σ interaction with ALA452; as well as π − alkyl interactions with VAL417, LEU420. Similarly, the compound showed π − σ interactions with ILE403 (**Figure 5.4**(**c**)). **ZINC000426406009** displayed conventional hydrogen bonding with ASP293, as well as π − σ interaction with PHE456. The compound made π − alkyl interactions LEU420, ILE403, MET365, while also showing π − π stacking interaction with PHE251 (**Figure 5.4**(**d**)).

The ligand **ZINC000020579927** displayed hydrogen bonding with TYR424 365, while ILE403 took part in π − σ interactions. PHE456 AND PHE441 showed π – π stacking interaction, while, LEU420 formed π − alkyl interactions with the ligand. (**Figure 5.4** (**a**)).

The bonding interactions of ligands **ZINC000001305675** and **ZINC000000377099** remained largely similar due to the identical core structures. So, the quinazoline core made the π – π stacking, π − σ as π – alkyl interactions while the secondary amine and the keto group participated in hydrogen bonding interactions. PHE251 and MET365 took part in van der Waals and alkyl interaction, respectively.

The ligand **ZINC000052245110**, comprising a different structure to that of the previous ligands, interacted with PDE9 by forming a hydrogen bond with His 252 through its hydroxyl group. The tetrahydro naphthalene moiety of this compound formed significant π – π stacking

and π – σ interactions at the residues PHE456, LEU 420, and VAL417, respectively. Here, the quinazoline moiety formed π – cation and π – alkyl interactions with MET365, ASP402 and HIS252 residues of the receptor.

The tetrazole moiety of **ZINC000426406009** showed hydrogen bonding with Asp 293 and an acceptor-acceptor interaction with Asp 402.Further, Leu 420, Ile 403 and Met 365 interacted with the receptor through a pi-alkyl bond. Ligand also interacted by forming pi-sigma bond, pi-cation bond, and pi-pi bond with Phe456, His 252and Phe251, respectively. The ligand **ZINC000020579927** showed conventional hydrogen bonding through Tyr 424 as well as pi-sigma interaction with Ile 403. Phe 224, Phe 441 and Phe 456 interacted with receptors by forming a pi-pi bond and Leu 420, Ile 403, and Phe 441 by forming pi-alkyl. The tetralin moiety formed the π – σ interactions, whereas, the phthalazine part of the molecule participated in the π – π stacking and π – alkyl interactions, the latter was shown by the methyl benzyl group as well. The hydrogen bonding interaction was carried out via the secondary amine.

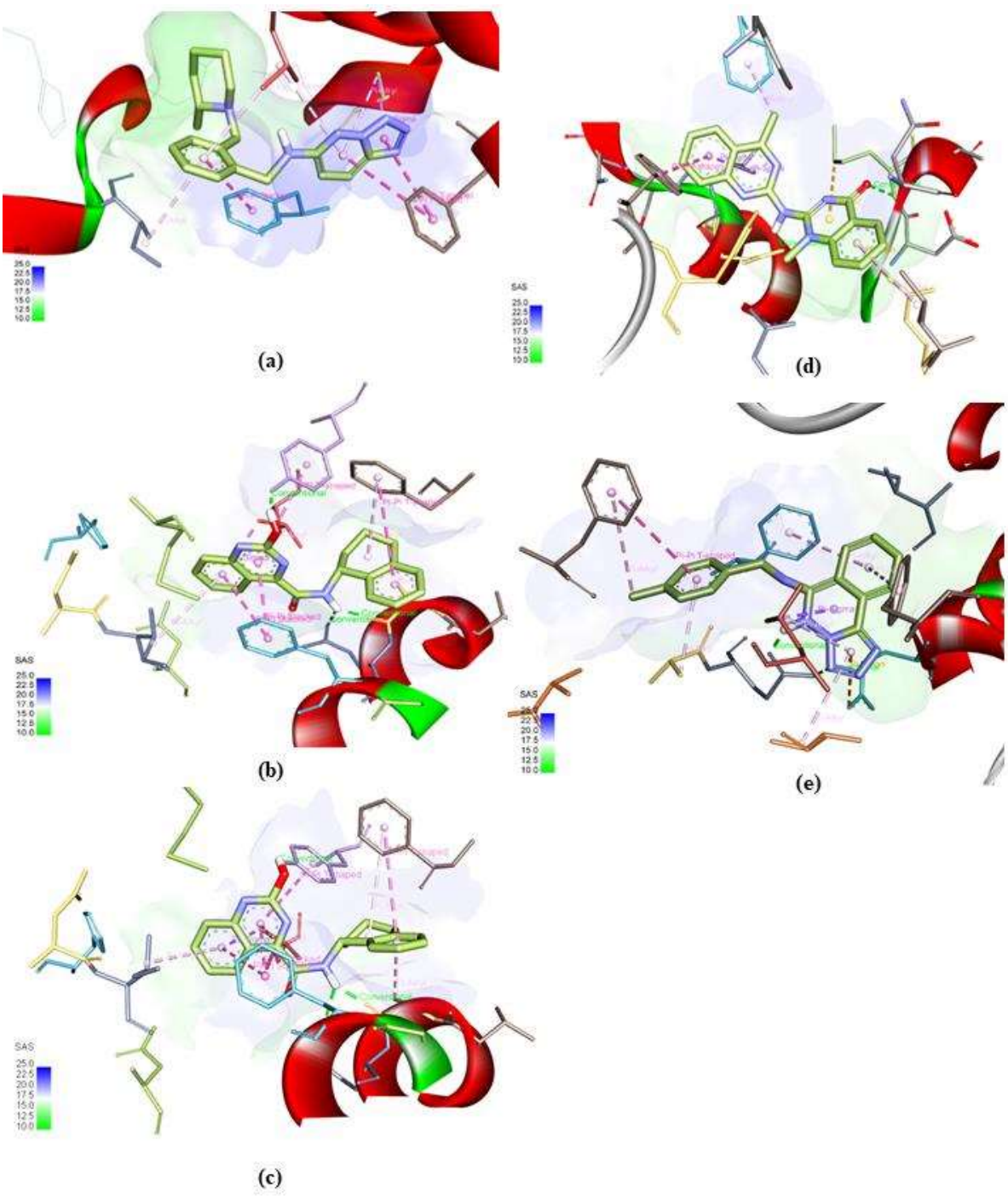

Figure 5.4 3D interactions of selected compounds (a) **ZINC000001305675** (b) **ZINC000000377099** (c) **ZINC000052245110** (d) **ZINC000426406009** (e) **ZINC000020579927**

5.3.7 ADMET properties

ADMET properties prediction is significant from the clinical point of view, to obtain a highly efficacious molecule with superior safety profile[127]. PreADMET server provides a convenient web interface for the prediction of numerous parameters, that are key to assess the pharmacokinetics of a drug candidate molecule [128, 129]. Adsorption becomes the limiting factor for the development of a drug molecule due to its effect on bioavailability and drug response [130]. Thus, a drug is considered as well absorbed if it shows human intestinal absorption (HIA) above 70%. The predicted HIA for five of the selected compounds was more than 94%, indicating high absorption capability of the molecules, among which **ZINC000052245110** showed the maximum HIA of 96.41 %. A Drug that targets the CNS must pass across the blood-brain barrier (BBB), which is determined by the ratio of drug concentration in the brain and blood. The Compounds having a BBB permeation ratio of more than 0.1 are considered BBB permeable or CNS active drug molecules. Three of the selected compounds had a BBB permeation ratio greater than 0.1 and were considered as CNS active. **ZINC000426406009** showed the highest BBB permeation of 0.817357. Aqueous solubility is also an important parameter and is considered in ADME prediction, as the poor solubility may lead to reduced potency. The aqueous solubility above 60 mg/L is deemed unsuitable for a drug with CNS activity [131]. **ZINC000052245110** showed the highest aqueous solubility as 393.595 mg/L, among the entire set of molecules selected for ADMET prediction. According to the PreADMET, **ZINC000001305675** showed maximum plasma protein binding as compared to all the selected molecules. Further, none of these compounds showed inhibitory effect on enzymes CYP_2C9 and CYP_3A4. **ZINC000426406009** and **ZINC000020579927** are the two compounds predicted as non-carcinogenic in rats and mice, among all the selected molecules.

Table 5.6 *In-silico* prediction of toxicities of selected compounds

Tests	ZINC000001305675	ZINC000000377099	ZINC000052245110	ZINC000426406009	ZINC000020579927
Algae_at	0.0168238	0.0286281	0.031689	0.0221114	0.05031
Carcino_Mouse	Negative	Negative	Positive	Negative	Negative
Carcino_Rat	Positive	Positive	Negative	Negative	Negative
Daphnia_at	0.0238854	0.0344213	0.146774	0.0254239	0.060858
hERG_inhibiton	Medium-risk	Medium-risk	Medium-risk	Medium-risk	Medium-risk
Medaka_at	0.00124348	0.00250422	0.037141	0.00135361	0.007395
Minnow_at	0.00210698	0.00460271	0.036302	0.00247014	0.016425
TA100_10RLI	Positive	Positive	Negative	Negative	Positive
TA100_NA	Positive	Positive	Negative	Positive	Negative
TA1535_10RLI	Negative	Negative	Negative	Negative	Negative

Table 5.7 *In-silico* prediction of ADME of the selected compounds

Properties	ZINC000001305675	ZINC000000377099	ZINC000052245110	ZINC000426406009	ZINC000020579927
BBB permeation	0.405378	0.6611	0.034046	0.817357	0.044643
PP Binding	98.39383	100	72.81081	90.35481	98.25306
CYP-2C19 inhibition	Non	Non	Non	Non	Non
HIA	96.13235	96.10054	96.41928	94.2495	96.18399

CYP-3A4 inhibition	Non	Non	Non	Non	Non
PGP inhibiton	Inhibitor	Inhibitor	Non	Inhibitor	Non
H_2O sol (mg/L)	0.144149	0.34999	393.595	1.35629	27.0027
MCDK	2.11368	34.6446	11.2696	171.631	23.8426
$CaCO_3$ cell line	22.4469	16.9102	22.0349	21.0272	20.3095
Log Sol pur H_2O	-6.36151	-2.93313	-5.95748	-5.37193	-4.03148
% PP binding	97.912057	72.810808	100	90.35481	98.253055

5.3.8 Molecular dynamics simulation studies

Molecular dynamics simulations pertaining to proteins were first developed in the early 1980s to utilize the developments in computing power in studying protein motion within its milieu. The dynamics studies are thermodynamic in nature and are generally studied as the changes in protein conformations and its coupled fluctuations. The most commonly used force fields for the protein energy surface parameterization are CHARMM, AMBER, and GROMACS with all the different force fields often generating consistent results for a given setting.

Proteins interact amongst themselves or with other small molecules or biopolymers in a dynamic manner to carry out their functions. Molecular Dynamics (MD) simulation studies provide detailed information about the motion and trajectory of the molecules in the presence of other molecules[115]. The study helps in analyzing various possible interactions and conformational changes within a system [112, 132]. Solvation of the molecules along with structural features of the protein and drug-protein interactions could be analyzed through MD.

In this study, two protein-ligand complexes of **ZINC000001305675** and **ZINC000000377099** were studied through MD simulations to establish the stability of the protein-ligand complexes. The detailed analysis of trajectories obtained from the MD run were analyzed for RMSD, protein RMSF, ligand RMSF, torsion profile, and hydrogen bonding.

Interactions between protein and ligand can be explained by PL-Contacts or LP-Contacts bar diagrams (**Figure 5.5**) for ligand molecules **ZINC000001305675** and **ZINC000000377099**. The diagram showed several specific and nonspecific interactions of the ligands with the amino acid residues of protein, further categorized as hydrogen bonds, hydrophobic, ionic, and water bridges.

(a)

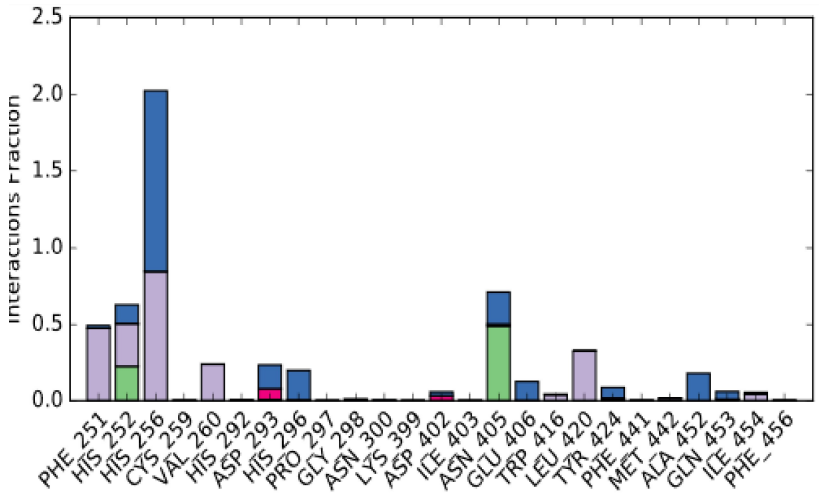

(b)

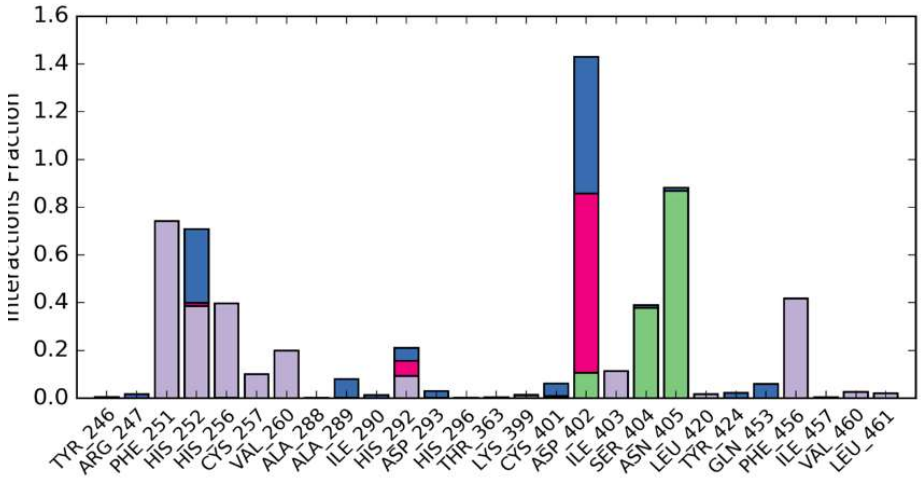

Figure 5.5 Bar diagrams of protein interaction with ligands (a) **ZINC000001305675** and (b) **ZINC000000377099** where, green represents H-bonding; gray, hydrophobic; blue, water bridges and pink represents ionic interactions.

In the protein-ligand interactions bar diagram, **ZINC000001305675** showed hydrogen bonding with HIS 256 and TYR 414, hydrophobic bonding with PHE 251, HIS252, LEU420, and PHE 456. However, ligand **ZINC000000377099** interacted by forming a hydrogen bond with HIS256 and hydrophobic bond with HIS252, MET 365, TYR 424, and PHE456. Protein-RMSD depicts the movements of different atoms of ligand present in the active site of receptor protein and provides deep insight into the structural conformations of the protein throughout MD simulation. The ideal deviation in RMSD for most globular proteins is considered to be in the range of 1–3 Å.

(a)

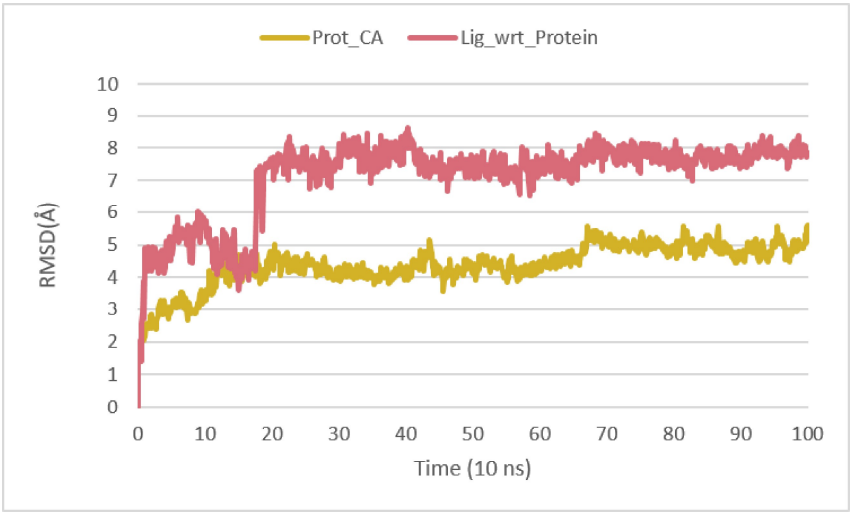

(b)

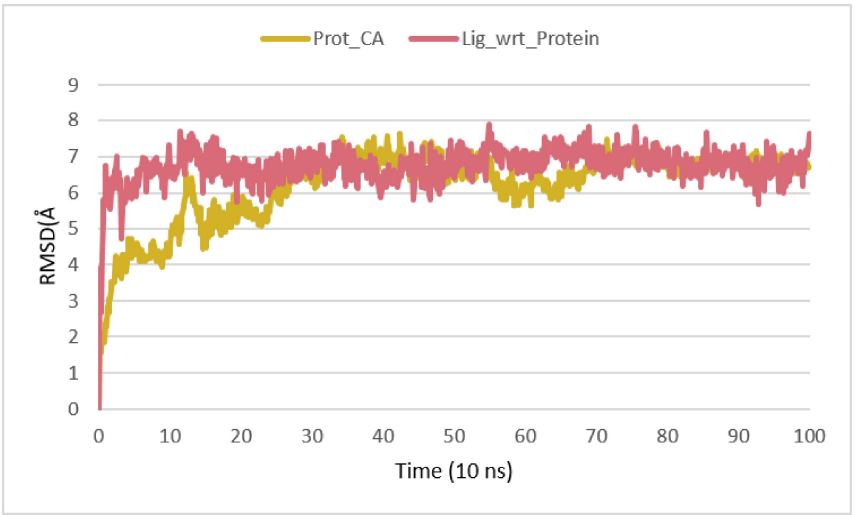

Figure 5.6 Protein RMSD for compounds (a) **ZINC000001305675** and (b) **ZINC000000377099**

RMSD analysis of **ZINC000001305675** protein complex had protein back bone RMSD of 3.47 Å, and ligand showed the average deviation of 0.4 Å and a maximum deviation of 3.855, whereas, **ZINC000000377099** protein complex displayed protein backbone RMSD of 3.05 Å and ligand showed the average deviation of 1.30 Å. In the ligand RMSD plot, the 'Lig fit prot' showed a smaller value than protein RMSD, may be the ligand is well diffused to the initial binding site and vice versa. But the trajectory of protein-ligand RMSD showed that ligand is well diffused with binding sites.

RMSF helps in predicting the structural integrity of the protein-ligand complex represented by RMSF graphs L-RMSF and P-RMSF. The P-RMSF describes local changes in the protein chain, whereas L-RMSF (**Figure 5.7**) describes changes in the positions of ligand atoms.

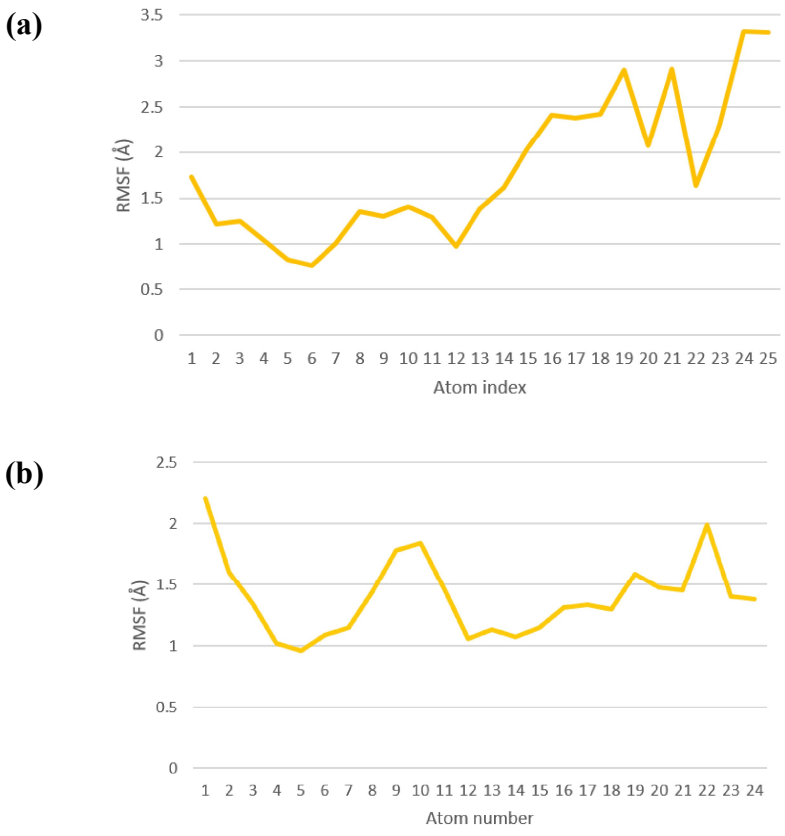

Figure 5.7 Ligand RMSF of selected compounds (a) ZINC000001305675 and (b) ZINC000000377099

Additionally, protein RMSF (P-RMSF) is used to measure the binding stability of the protein by observing the fluctuations in peaks of the plot during simulation.

The average P-RMSF was found to be 2.54 and 1.85 Å for **ZINC000001305675-protein** and **ZINC000000377099-protein** complexes, respectively. The ligand RMSF showed per atom ligands fluctuation. The average ligand RMSF for **ZINC000001305675** and **ZINC000000377099** was found to be 0.3596 and 0.574 Å, respectively.Ligand torsion is an essential parameter to study the thermodynamic function of ligand binding free energy, with the number signifying the flexibility of the same. The conformational changes that each rotatable bond (RB) present in the ligand molecule undergoes throughout its MD simulation could be described from its ligand torsion profile. In **Figure 5.8**, the various rotatable bonds within the ligand structure are color-coded differently and represented by means of a dial plot and a bar plot shown in colors corresponding to the respective bond [133]. While the bar plot represents the probability of torsions as a function of angle, the dial plot displays the torsional angle as coordinates growing radially outwards throughout the simulation. **ZINC000001305675** showed the presence of two rotatable bonds between ligand atoms 14-13 and 13-04, and **ZINC000000377099** showed two rotatable bonds between ligand atoms 13-12 and 12-04.

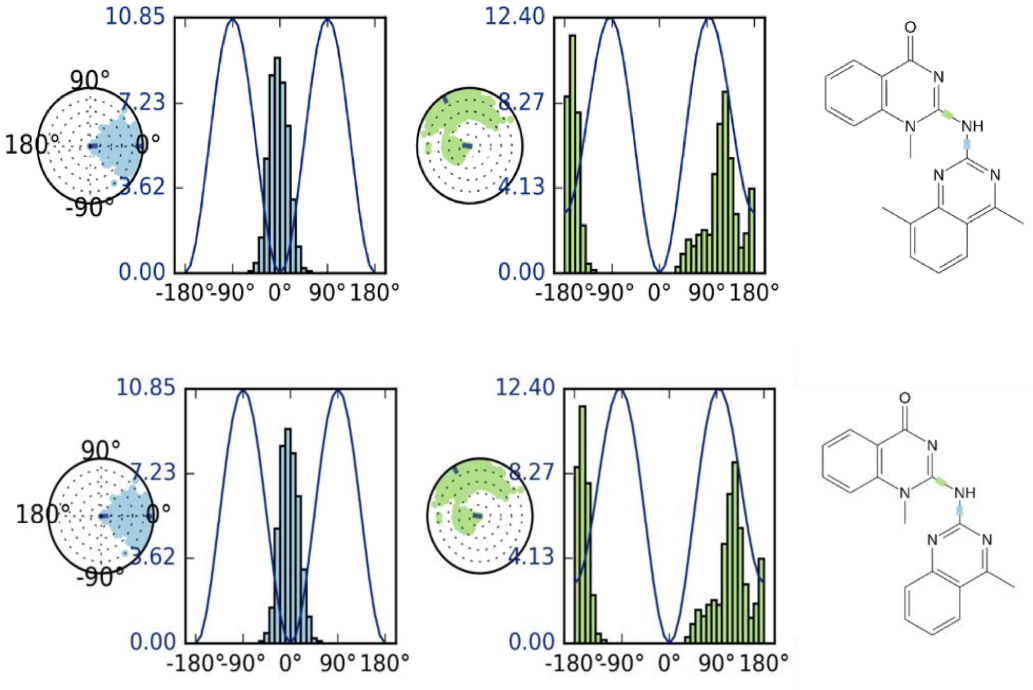

Figure 5.8 Torsion profile of selected ligands **ZINC000001305675** and **ZINC000000377099**

Hydrogen-bonding properties must be taken into account while developing new drugs since H-bonds, or hydrogen bonds, have significant impact on drug specificity, metabolization, and adsorption due to their effect on ligand binding. The four subtypes of hydrogen bonding seen in protein ligand binding are, backbone acceptor, backbone donor, side-chain acceptor, and side-chain donor. **ZINC000001305675** showed H-bond interactions with the residues ASN 405, ASP 293, GLN 453, HIS 252, and TYR 424 while, **ZINC000000377099** showed H-bond interactions with the residues ASN 405, ASP 402, CYS 401, HIS 256, and SER 40. (**Figures 5.9 & 5.10**)

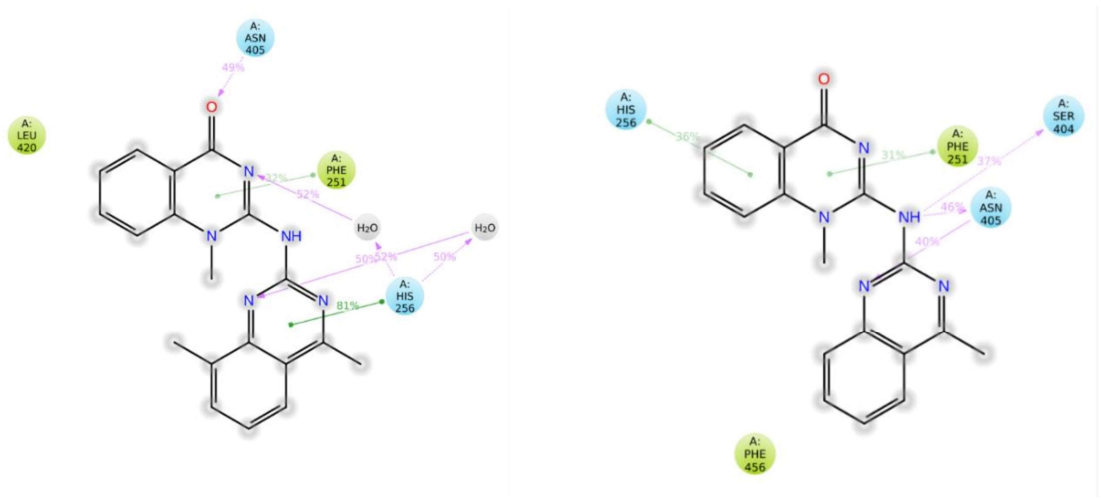

Figure 5.9 Hydrogen bond interactions of the selected ligands **ZINC000001305675** and **ZINC000000377099**

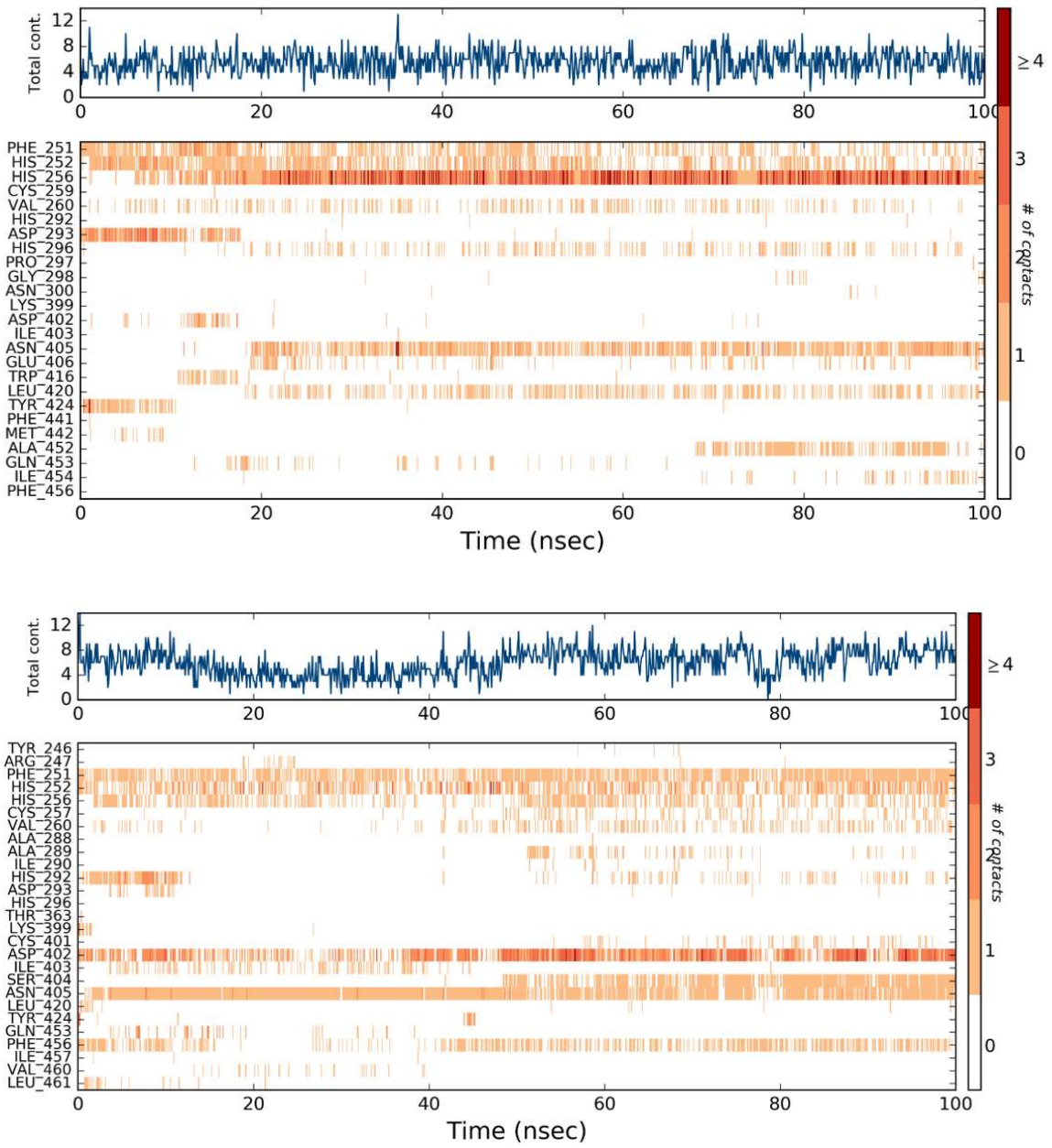

Figure 5.10 Ligand-protein contacts of the selected ligands **ZINC000001305675** and **ZINC000000377099**

Solvent accessible surface area (SASA) was calculated by using a probe of van der Waals radii of 1.4 Å. The average SASA for each of the complete MD simulations of the compounds, **ZINC000001305675** and **ZINC000000377099** against PDE 9 was found to be 120.74 and 86.19 Å respectively. It was observed that there was a decrease in SASA values after ligand binding in the case of **ZINC000000377099** (**Figure 5.11**).

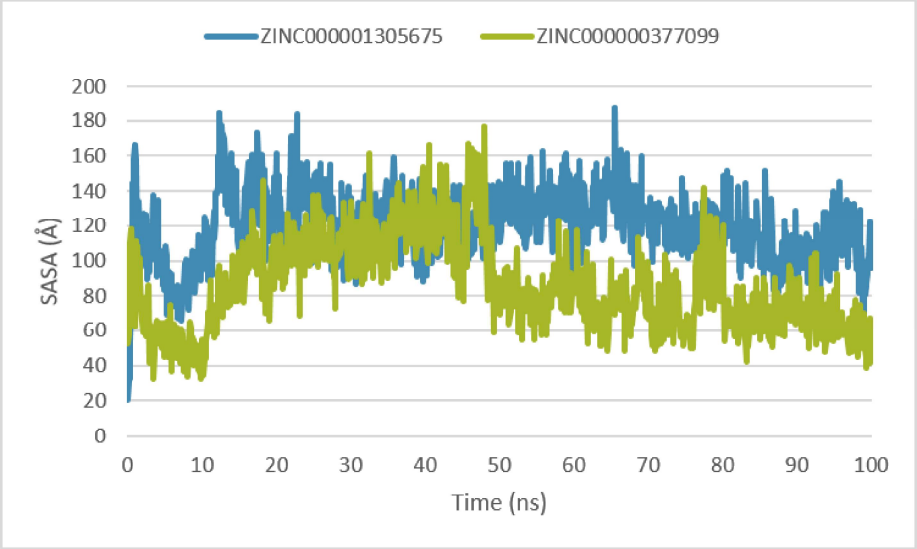

Figure 5.11 SASA (Å) selected ligands (a) **ZINC000001305675** and (b) **ZINC000000377099**

The radius of gyration (rGyr) indicates the compactness of the interaction. A lower rGyr value could be correlated with having higher stability and vice versa. rGyr vs time plot of both the compounds can be seen in Figure 12. The average rGyr was found to be 4.09 Å and 4.06 Å for **ZINC000001305675** and **ZINC000000377099** respectively, during an MD run of 100 ns. The radii were comparable for both the compounds (**Figure 5.12**).

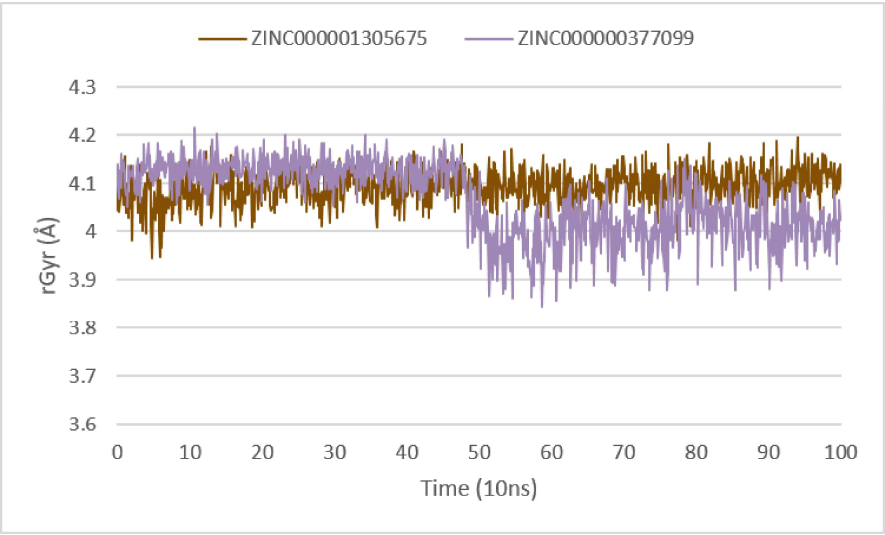

Figure 5.12 Radius of Gyration, r_{Gyr} (Å) for selected ligands (a) **ZINC000001305675** and (b) **ZINC000000377099**

5.4 Conclusion

The understanding of protein-ligand binding has been greatly benefited from computational biology and molecular modelling. Drug discovery has become substantially less expensive due to the application of molecular modelling techniques. PDE9, an abundantly expressed enzyme in the cortex of the brain as well as in the hippocampal region, is involved explicitly in the maintenance of cGMP levels through its hydrolysis. As cGMP is essential for synaptic plasticity and neuronal transmission, a drug that inhibits the PDE9 enzyme and subsequently increases the levels of cGMP may be promising for the management of AD. The study deals with the *in-silico* study executed to identify potential PDE9 inhibitors. Seven different structure-based pharmacophore models were developed from 9Q9, a PDE9 inhibitor complexed with the 3D structure of the protein (PDB 6A3N). Pharmacophore-based screening of the ZINC database followed by PAINS, and drug-likeliness filtration were carried out. The hits so obtained were further ranked using protein-ligand docking interaction studies, binding energy calculations, ADMET analysis, and MD simulation. Molecular docking-based virtual screening was used to identify compounds with a binding energy of >-10 kcal/mol, which were then subjected to *in-silico* pharmacokinetics and toxicity screen to ascertain potential clinical candidature. A molecular dynamics simulation run of 100ns was performed on two molecules, namely, **ZINC000001305675** and **ZINC000000377099**, which showed the highest binding affinities of -10.90 and -10.30 Kcal/mol, respectively. The study revealed that both the hits showed minimal fluctuations in PL-RMSD and L-RMSF and possessed excellent physicochemical characteristics. Thus, **ZINC000001305675** i.e., (2-((4,8-dimethylquinazolin-2-yl) amino)-1-methylquinazolin-4(1H)-one) and **ZINC000000377099** i.e., (1-methyl-2-((4-methylquinazolin-2-yl) amino) quinazolin-4(1H)-one) may be considered as worthy candidates for *in-vivo* and *in-vitro* studies targeting PDE 9 enzyme for AD and further exploration.